Journal of Materials Research and Technology 39 (2025) 4963–4972

Contents lists available at ScienceDirect

Journal of Materials Research and Technology

journal homepage: www.elsevier.com/locate/jmrt

Enhanced mechanical and thermomechanical performance of basalt–carbon hybrid composites reinforced with titanium wire mesh

E.S. Esakkiraj [a], Sikiru O. Ismail [b], Rajini Nagarajan [c,*], Faruq Mohammad [d], Kumar Krishnan [e], M.P. Indira Devi [f]

[a] Department of Mechanical Engineering, Dambi Dollo University, DambiDollo, Ethiopia
[b] Centre for Engineering Research, School of Physics, Engineering and Computer Science, University of Hertfordshire, Hatfield, Hertfordshire, AL10 9AB, United Kingdom
[c] Department of Mechanical Engineering, Kalasalingam Academy of Research and Education, Krishnankoil, 626126, India
[d] Department of Chemistry, College of Science, King Saud University, P.O. Box 2455, Riyadh, 11451, Kingdom of Saudi Arabia
[e] INTI International University, Persiaran Perdana BBN, 71800, Nilai, Negeri Sembilan, Malaysia
[f] Department of Physics, Ramco Institute of Technology, Rajapalayam, 626117, India

ARTICLE INFO

Handling Editor: SN Monteiro

Keywords:
Carbon fiber
Basalt mineral fiber
Metal wire mesh
Metal fiber laminate
Mechanical/thermomechanical properties:
Producct innovation

ABSTRACT

This study focused on development of innovative metal fiber polymer laminates (MFPLs) for high-impact load-absorbing applications in automotive, aerospace and soundproofing. Therefore, a woven titanium (Ti) wire mesh was used as the highimpact load absorber and highductility reinforcement of the fabricated MFPLs, using hand layup and compression molding methods. The MFPLs comprised both carbon (C) and basalt (B) fibers reinforced polymer (FRP) hybrid composites in various stacking sequences.The mechanical (tensile, flexural and impact) and thermomechanical (dynamic mechanical analysis: tan delta/damping, storage and loss moduli) properties of the various B/C/Ti MFPLs were examined. From the experimental results obtained, sample TiC6Ti recorded maximum tensile and flexural strengths of 612and 762 MPa, respectivelywhen compared with other B/C/Ti MFL hybrid composite samples. Additionally, sample TiBCBCBCTi recorded the highest flexural strength among the basalt fiber-based MFL hybrid composite samples. However, samples C3Ti2C3 without basalt fiber and TiC6Ti exhibited the lowest and highest impact strengths of 149 and 166 kJ/m^2 when compared with other samples, establishing the negative effect of absence of basalt fiber on the Ti MFL composite systems. Besides, according to the dynamic mechanical analysis (DMA) results, sample TiC6Ti recorded maximum storage and loss moduli of 28185.20 and 5333.60 MPa, respectively and lowest damping property/tan delta value of 0.45. Summarily, the innovativeand optimal stacking sequenced sample B/C/TiMFPLs exhibited promising mechanical and thermomechanical properties for appropriate high-impact, structural and load-absorbing applications.

1. Introduction

Composites made of fiber-reinforced polymer (FRP) matrix are widely used in structural industries, such as construction, marine, defense, aerospace and automotive. These various applications can be associated with their excellent load-bearing capacity, availability and cost-effectiveness. Among various reinforcement techniques, fiber strengthening stands out as a highly promising method for developing high-strength polymer matrix composites (PMCs), making it suitable for a wide range of engineering applications [1–3]. Due to their remarkable strength and stiffness, as well as their capacity to improve the structural characteristics of polymer composites, synthetic fibers are widely used in a range of industries. Basalt, carbon and Kevlar are among the most frequently used synthetic fibers, each providing distinct benefits. Carbon fiber is especially significant for highperformance applications, including military gear, car parts, building construction materials, wind energy systems and aircraft manufacturing. Its superior strength-to-weight ratio, durability and resistance to corrosion make it an ideal choice for the afore mentioned sectors [4–6,41]. Despite of the exceptional characteristics of carbon fiber, the use of carbon fiber-reinforced polymer (CFRP) is still quite restricted [7,8]. This limitation is primarily due to some challenges, such as high production costs, difficulties in recycling and the need for specialised manufacturing processes [9,10].

* Corresponding author.
E-mail address: rajiniklu@gmail.com (R. Nagarajan).

https://doi.org/10.1016/j.jmrt.2025.10.155
Received 30 August 2025; Received in revised form 9 October 2025; Accepted 19 October 2025
Available online 20 October 2025

The hybridisation of reinforcement in the polymer composite system overcomes these limitations [11]. Additionally, several studies have demonstrated that hybridisation reduces the restrictions, while enhancing mechanical and thermomechanical capabilities. The combination of high-strength and shock-dissipating fibers largely determines the structural characteristics of a composite [12–15]. Basalt fiber is another mineral-based reinforcement and it is a less expensive and mostly environmental alternative to synthetic fibers. It is also classified as a high-strength natural fiber. Basalt fiber exhibits high thermal stability, significant water resistance and excellent electrical insulation qualities. Several research have established that incorporating basalt fiber layers in a composite system significantly enhances the mechanical strength and stiffness of the PMCs. Moreover, the remarkable resistance to water, superior thermal stability and appealing electrical insulation characteristics of basalt fiber make it an attractive choice for various applications [16–18]. Although basalt fibers offer environmental benefits, the inclusion of epoxy and titanium mesh limits full recyclability. However, titanium's high recovery rate and the open-mesh architecture enable efficient metal reclamation after thermal or chemical matrix removal. Future improvements could include substituting epoxy with reprocess able or bio-based matrices and adopting layer-selective adhesives for easier disassembly. Thus, while it is not fully recyclable, the developed tri-hybrid basalt–carbon–titanium (B/C/Ti) metal fiber polymer laminates (MFPLs) represent a transitional step toward sustainable highperformance hybrid laminates.When basalt fibers are added to thermoset polymer resins, such as epoxy, polyester and vinyl ester, the mechanical properties of the resulting composites are significantly enhanced [11,19,20].

Furthermore, polymer composites are often created by layering different types of fibers or incorporating additional fiber materials into the mixture. The type of reinforcement, quantity of fiber stacking layers, placement and orientation of fiber, the fiber-matrix interfacial adhesion or bond, the amount of fibers present and the manufacturing process impact the demanding properties of hybrid composites. The improved mechanical behavior of woven fabric stacking hybrid polymer composites over randomly fiber composites has been reported in numerous research [14,21,22]. The location of both high and low strength fibers influences the mechanical properties of polymer composites.Fibers stacking levels and locations have a significant effect on both physical and structural features, especially on the outer and inner core fiber layers [23]. Aabdul Khalil et al. [24] explored how the sequencing of laying of palm oil and glass fiber impacts the mechanical characteristics of a polymer laminate.Six fiber material layers were used to create each hybrid composite. Using glass as an outer covering in the stacking configuration was proposed to increase strength and flexural capabilities significantly. Skin of tough synthetic glass fibers tolerated more bending strength.

It is a common practice to use thermomechanical testing or dynamic mechanical analysis (DMA) to assess the viscoelastic properties of polymeric composites, namely; tan delta (TD) or damping behavior, storage modulus (SM) and loss modulus (LM). These characteristics offer important information about the material's capacity to absorb and release energy under dynamic loading conditions. Many investigation results revealed that adding fibers to the polymer matrix greatly improves the composite's mechanical strength and storage modulus. This improvement is credited to the capacity of the fibersto restrict polymer chain mobility, which raises the stiffness and load-bearing capacity of the composite material [25–27].Thethermomechanical properties of a polymer compositeare also influenced by the placement and arrangement of its various fibers.The viscoelastic characteristics of PMCs are examined at various temperatures. Hybridized composites exhibit highly unpredictable characteristics in the transverse plane, because the heat flow path is orthogonal to the fiber orientation [28]. Dynamic mechanical properties of individual/mono fiber content-loaded composites are inferior to that of hybridized composites. According to Romanzini et al. [29], the combination of ramie with glass fiber caused dynamic mechanical properties of the polymer lamination to increase more [29]. Given that the addition of high strength fibers increases the rigidity of the composite, this could explain the observed effects. Several studies have reported that hybridizing synthetic and natural fibers with epoxy composites improves the storage modulus when compared with a pure epoxy sample [30]. Additionally, research suggests that carbon fiber, which is stiffer than basalt fiber, further enhances dynamic characteristics, including storage and loss moduli. Studies agree with the above highlights; hence, the need for sustainable, green material for structural implementation. FRP design, which involves stacking fiber plies separately or in conjunction with a ply angle, significantly impacts the selection of composites with good physical and damper structural properties.Variable fiber fabric layering patterns in polymer composites increase its flexibility, flexural strength and breaking abilities. Conversely, the process of hybridizing metal with composite layers forms fiber metal laminates (FMLs). The concept of replacing the metal sheet with layers of woven metal fiber may also provide or demonstrate various advantages. An appropriate adhesive method is used to bond together alternating composite and metal fiber layers to form FMLs. They combine the advantages of metal alloys and composites with fiber reinforcement, while avoiding the disadvantages of each used alone. The most often used metals in FML are copper, steel, titanium and aluminium [31,32]. The advanced new stacking design of (FML) is widely used in various applications, such as aircraft, civil and marine industries, among others, due to their superior properties: impact, high strength-to-weight ratio, fatigue and other structural properties. High strength metals, such as magnesium alloy, aluminum alloy, titanium and grade types of steel in thin sheets are well known to be used in the FML [33,34].The load-bearing capacity and uniformity are two different cases and the uniformity is highly dependent on the fiber arrangement in the composites. High velocity load absorption abilities may be crucial for PMCsemployed in industrial settings, where fibers or metal wire mesh may act as impact load absorbers [35,36]. Botelho et al. [37] investigated into the natural frequency characteristics of aluminum alloy, carbon fiber/epoxy, glass fiber/epoxy and their hybrid MFLs (aluminum alloy/carbon fiber/epoxy and aluminum alloy/glass fiber/-epoxy) and discovered that MFLs demonstrated greater natural frequency than FRPs. Studies agree with the above highlights; hence, the need for sustainable, high-performance materials. Recent work has advanced this field: Huang et al. [38] reviewed kenaf fiber-reinforced biocomposites for marine applications, emphasizing their mechanical performance and eco-friendliness. Shelly et al. [39] examined bio-based fiber-reinforced polymer composites, highlighting strategies to improve strength and durability. Ghafar et al. [40] developed a mobile robot for precise fertilizer and pesticide spraying, showing the role of intelligent systems in modern engineering applications. These studies reflect the trend toward combining sustainable, high-performance materials with functional innovation, providing context for the development of tri-hybrid B/C/TiMFPLs with superior mechanical and thermomechanical properties.

The present study introduced a novel tri-hybrid B/C/Ti composite system, establishing a new class of MFPLs with superior mechanical and thermomechanical performance. Unlike previous basalt–carbon hybrid composites that used only fiber reinforcements, this work uniquely integrated a woven titanium wire mesh, as a ductileand highimpact reinforcement layer. The use of woven Ti mesh, rather than flat metal sheets, enhanced interfacial adhesion, delamination resistance and energy absorption. Through systematic optimization of four stacking configurations (MFL-I to MFL-IV), the study demonstrated how the placement of Ti, carbon and basalt layers influenced strength, stiffness and damping properties. This work therefore advanced beyond existing basalt–carbon hybrids by creating a functionally graded, high-strength and vibration-damping laminate suitable for impactresistant applications in aerospace and automotive sectors, marking a clear and measurable step forward in hybrid composite design.It is evident from the extensive literature studied that the development of environmentally friendly, high-strength FMLs with enhanced vibration behavior for various structural applications is lacking. The effects of titanium skin and basalt layers intertwined with carbon fiber on the mechanical properties and energy absorptive capabilities of FMLs have not been extensively explored previously. Therefore, this study is essential in an attempt to bridge the research gap. Consequently, this research focused on development of advanced FMLs. The developed FMLs were tested according to American Society for Testing and Materials (ASTM) standards. The failure behaviors of the fabricated FMLs were examined, using scanning electron microscopy (SEM) technique. The newly developed high-strength,energy-absorbing, environmentally friendly FMLsdemonstrated potential for applications in the manufacture of airplane parts, helmets, automobile bumpers and boat hulls, where a combination of high strength and damping is essential.

Furthermore, studies indicate a growing demand for FML composites with suitable mechanical strength and damping capabilities. Hence, this research also supportsfabrication of a composite laminate with excellent stability and damping properties.The dynamic properties of the developed FML composites, such as damping ratio, loss modulus and storage modulus were investigated and subsequently elucidated.

2. Materials and methods

The objective of this study focused ondesign and development of high performance, environmentally friendly FMLs. Therefore, subsequent materials were chosen, considering their exceptional mechanical qualities and environmental advantages.

2.1. Materials

The epoxy resin utilized in this study was Araldite LY556, which has an average density of 1.10 g/cm^3. Triethylenetetramine (TETA), an aliphatic amine hardener with a density of 0.98 g/cm^3 was used as the curing agent. The epoxy resin and curing agent were mixed in a weight ratio of 10:1, as recommended for optimal cross-linking and mechanical performance. The reinforcements employed in the fabrication of the composite laminates included woven basalt and carbon fiber fabrics, both sourced from Go Green, Chennai, along with titanium mesh obtained from a local steel shop in Chennai.

2.2. Manufacturingmetal fiber laminates

A laminate composed of titanium (Ti) wire mesh, carbon fiber, basalt fiber and epoxy resin was fabricated, using the compression molding technique.Titanium was chosen over aluminium or magnesium alloys because of its higher specific strength, superior corrosion and thermal resistance, and better chemical compatibility with carbon fibers. The use of woven Ti wire mesh enhanced interfacial adhesion and impact energy absorption in comparison with flat aluminium or magnesium sheets. Although a detailed cost or environmental assessment was not conducted within the scope of this study, the material selection was performance-driven to achieve optimal stiffness, strength and damping synergy within basalt–carbon hybrid laminates, with probably long-term cost benefit.To increase the surface roughness of titanium mesh and improve its adhesion to the polymer laminate, sandblasting was carried out.Fig. 1 shows the Ti mesh location and layer arrangements of the various MFL composites. Afterwards, an annealing process was carried to eliminate any residual stress developed during the sandblast operation, titanium surface treatment and chemical element analysis (Fig. 2).Sandblasting and annealing were performed to enhance Ti–epoxy adhesion. Initially, a hand layup method was employed to arrange and assemble the layers of the materials, forming the MFL compositesamples. To minimize environmental variability during the sunlight curing stage, all composite samples were exposed under controlled and consistent conditions. The preliminary curing was performed under clear sky conditions for a total of 24 h, with an average ambient temperature of 30 ± 2 °C and relative humidity of 55 ± 5 %. The laminates were placed within a transparent acrylic enclosure to prevent the influence of wind, dust and direct moisture exposure, thereby maintaining uniform curing conditions. The purpose of sunlight curing was to enable initial resin gelation and solvent release prior to the controlled thermal post-curing stage. All samples were prepared using identical resin batches, mixing ratios and lay-up procedures to ensure process uniformity. Subsequently, post-curing was conducted in a furnace at 60 °C for 1 h to complete cross-linking under a stable thermal environment. This two-step curing approach allowed for consistent pre-polymerization during sunlight exposure, while ensuring reproducible final mechanical and thermomechanical performance across all laminate configurations.The composites comprised various woven layering configurations, designated as MFL-I, MFL-II, MFL-III and MFL-IV.Table 1 presents details on the specific arrangements of woven layers, as well as the corresponding weight percentages of the matrix and the fibers. In the

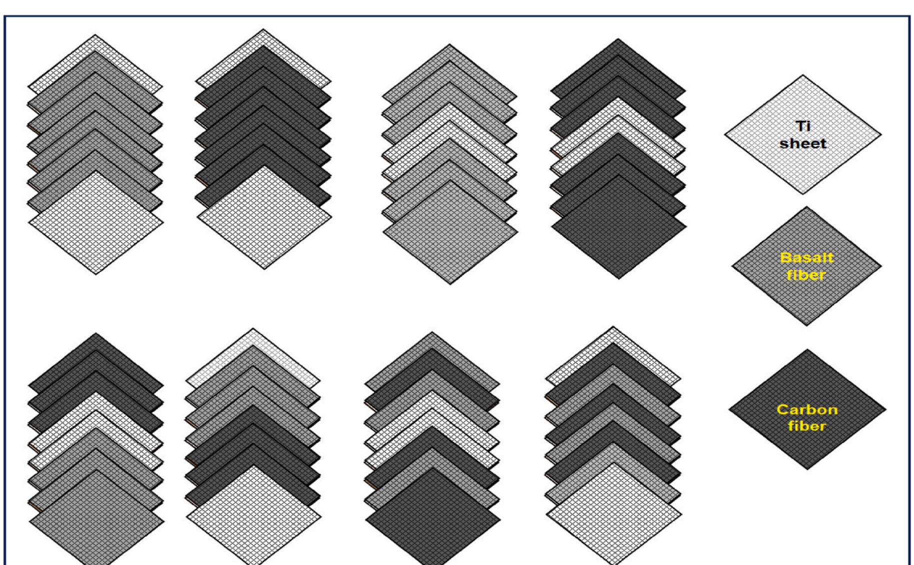

Fig. 1. Ti mesh locations and layer arrangements of the various MFL composite samples.

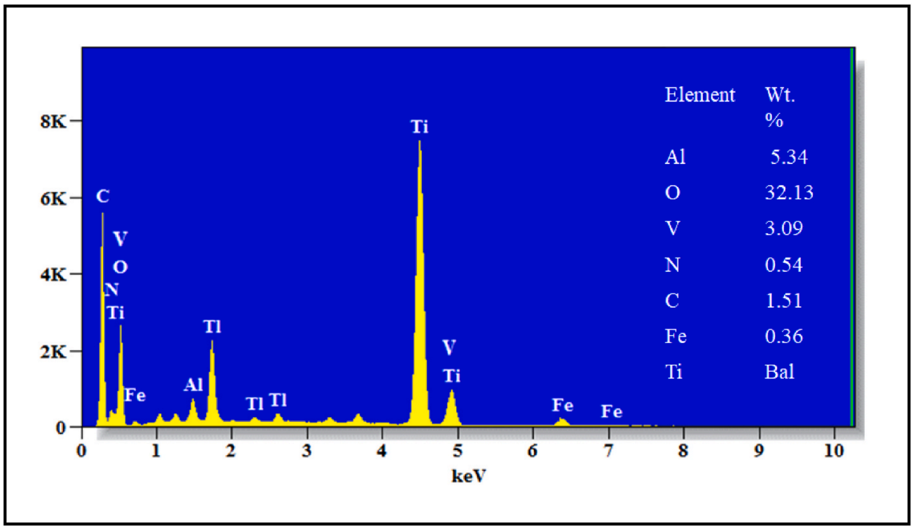

Fig. 2. EDX analysis of titanium mesh.

Table 1
Types of the various MFL composite samples used.

Description	Type of layering composites	Fiber layering arrangement
MFL-I	TiB6Ti	Core basalt layers (Ti skin layers)
	TiC6Ti	Core carbon layers (Ti skin layers)
MFL-II	B3Ti2B3	Skin basalt layers (Ti core layers)
	C3Ti2C3	Skin carbon layers (Ti core layers)
MFL-III	B3Ti2C3	Skin basalt and carbon layers (Ti core layers)
	TiB3C3Ti	Core basalt and carbon layers (Ti skin layer)
MFL-IV	CBCT2BCB	Alternative fiber layers (Ti core layers)
	TiBCBCBCTi	Alternative fiber layers (Ti skin layers)

fiber arrangement nomenclature, titanium wire mesh, woven carbon and basalt fiber were denoted as Ti, Cand B, respectively. Fig. 1 depicts different woven overlaying configurations (MFL-I to MFL-IV) as well as the appearance of their manufactured intertwined composite samples.

2.3. Mechanical tests

ASTM D638 standard was used to fabricate dog bone-shaped tensile MFL samples. These samples were tested for tensile strength (TS) with aid of Universal Testing Machine (UTM) equipped with pair of gripping devices. The sample was placed between the grippers, and the movable end was extended at a constant strain rate of 5 mm/min. A standard procedure for tensile testing and fractured samples were used. Besides, flexural MFL samples were prepared according to the ASTM D790 standard [21], using a 3-point bending configuration on the UTM. For each test condition, the deviation from the mean was calculated based on the results of five samples. Although five replicates per condition satisfied ASTM testing requirements, the inherent variability of hand lay-up fabrication may influence data scatter. The low standard deviations of <5 % obtained suggested good reproducibility; however, increasing the number of replicates and employing statistical modeling (such ANOVA or Weibull analysis) would enhance confidence and reliability. Future studies will use controlled lay-up techniques and larger datasets to reinforce statistical significance.The tensile fracture surfaces and failure mechanisms of the composites were examined, using SEM. An accelerating voltage of 5 kV (JOEL JSM840A) and extra electron contrast mode were used for the SEM. To create a conductive surface, the polymeric composite samples were gold-sputtered. Also, impact test MFL samples were prepared according to the ASTM D256 standard. The typical mechanical testing standards and the MFL sample setup are depicted in Fig. 3.Young's modulus and elongation values were not explicitly tabulated, as the study primarily compared strength and thermomechanical trends across stacking sequences.

2.4. Dynamic mechanical analysis

DMA was employed to investigate the viscoelastic properties of various polymeric composite layering configurations, following ASTM D4065-01 standards. The samples used for testing measured 50 × 10 mm^2. The DMA experiments were carried out using the twin cantilever mode of the NETZSCH DMA-242 instrument. During the test, the samples with different stacking configurations were heated from room temperature up to 200 °C at a constant heating rate of 2 °C/min. Dynamic properties, including the SM, LM and TD were recorded at different frequency levels, beginning at 1.0 Hz. These dynamic parameters were computed based on the data collected by the data logger integrated with the DMA system.

3. Results and discussion

3.1. Tensile strengths and fractured surface analysis of the MFL composites

The effect of various stacking configurations of fibers on the tensile strength of natural basalt interlaced carbon fiber composite samples MFL-I, –II, –III and -IV is shown in Fig. 4.The composite with a pure carbon core and a Ti mesh outer layer (TiC6Ti) exhibited the highest tensile strength among the MFL composites, due to the superior strength of carbon fiber [26].The tensile strengths of MFL-I and MFL-II composites, which depended on the type and position of fabric layers of basalt, carbon and titanium, were significantly influenced by their stacking sequences. The TiC6Ti composite, comprising high-strength carbon fiber layers, demonstrated higher tensile strength than the TiB6Ti composite, which had a basalt fabric core and a titanium mesh skin. Notably, the TiC6Ti woven layering arrangement exhibited a 111 % increase in tensile strength when compared with the TiB6Ti composite.For the MFL-II design, the tensile strength was strongly affected by the outer woven skin layer. A similar trend was observed in carbon-stacked Ti composites, which exhibited higher tensile strength than basalt-stacked Ti composites. The tensile (612 MPa) and flexural (762 MPa) strengths of the TiC$_6$Ti laminate are comparable to or exceed those of conventional aluminium-based FMLs (450–600 MPa) and approach lower-range aerospace-grade CFRPs (550–900 MPa). Its

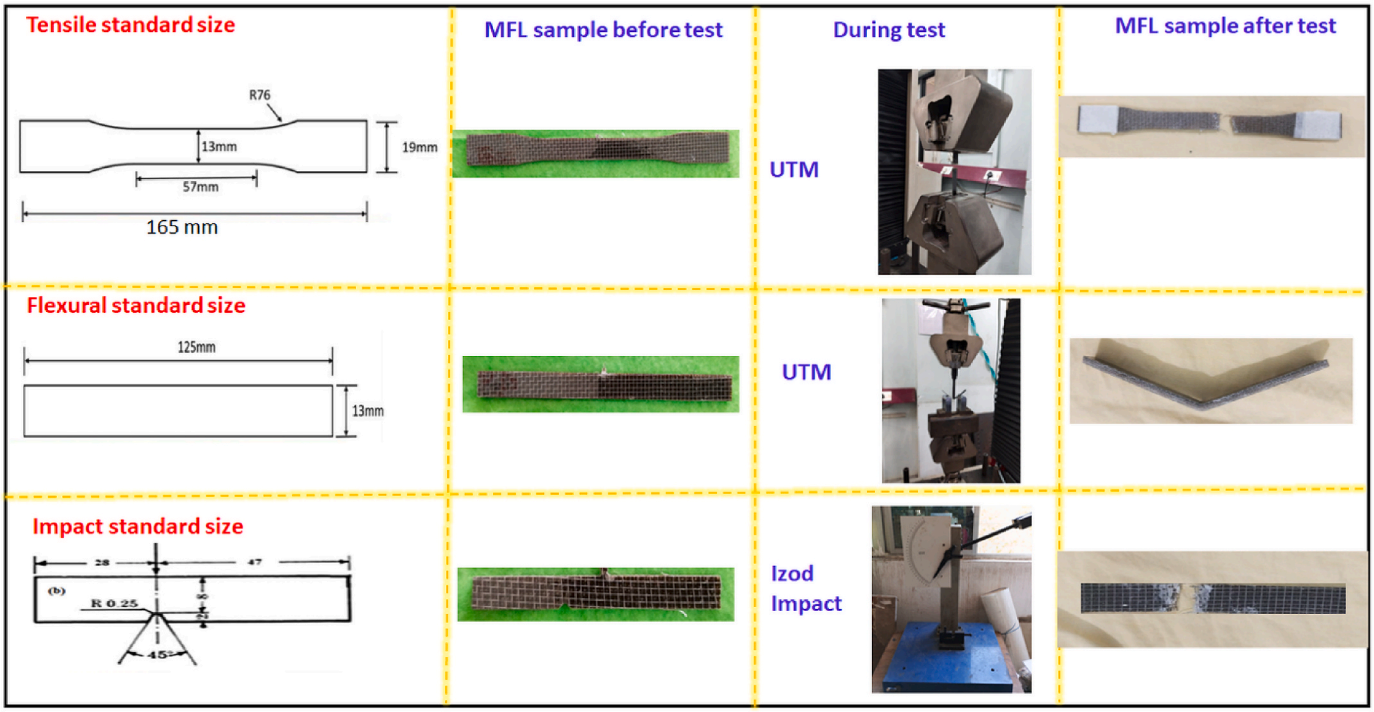

Fig. 3. Mechanical test standards and their samples.

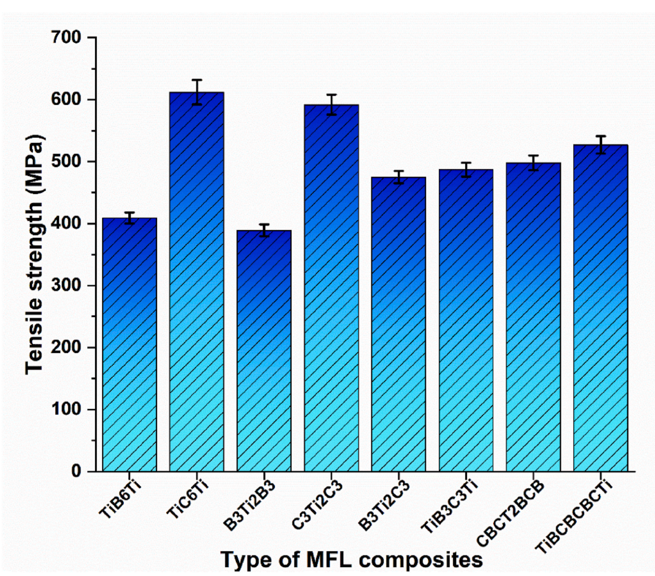

Fig. 4. Tensile strengths of various stacked MFL-I, II, III & IV polymer composite samples.

higher storage modulus (28.2 GPa) and improved damping behavior (tan δ = 0.45) indicated competitive stiffness and vibration suppression. These results position the developed B/C/Ti MFPLs as a promising alternative to current CFRP and FML materials, particularly for high-impact andthermal resistant materials that are highlyrequired in aerospace and automotive applications.

However, composites with a Ti core showed a reduction in tensile strength. In case of MFL-III and MFL-IV hybrid fiber-stacked composites, tensile strengths varied based on the core and fiber positions. The TiBCBCBCTi composite, with an interwoven laminate, exhibited higher tensile strength when compared with B3Ti2C3, TiB3C3Ti and CBCTi2CBC stacking configurations. Among these categories, the CBCTi2CBC composite demonstrated superior tensile strength when compared with B3Ti2C3 and TiB3C3Ti.The increased strength in alternative fiber stacking patterns can be attributed to strong interfacial adhesion. These findings align with previous studies on high-strength fiber-epoxy composites, which also exhibited enhanced tensile properties similar to the studied stacking configurations that utilized E-glass fiber as an external skin layer [23].

Based on weave layers stacking configurations, Fig. 5 depicts the typical stress-strain behaviors of the various MFL composites. The stress-strain observations of the C/B/Ti hybrid composite revealed two distinct slopes in the tensile phase. Initially, the matrix and fibers jointly resisted the tensile force, resulting in a steeper first slope [34,35]. Fracture analysis showed that the carbon fiber layer fractured first, due to its lower elongation when compared with basalt fiber, regardless of its stacking position. Stress concentration around the broken carbon fibers

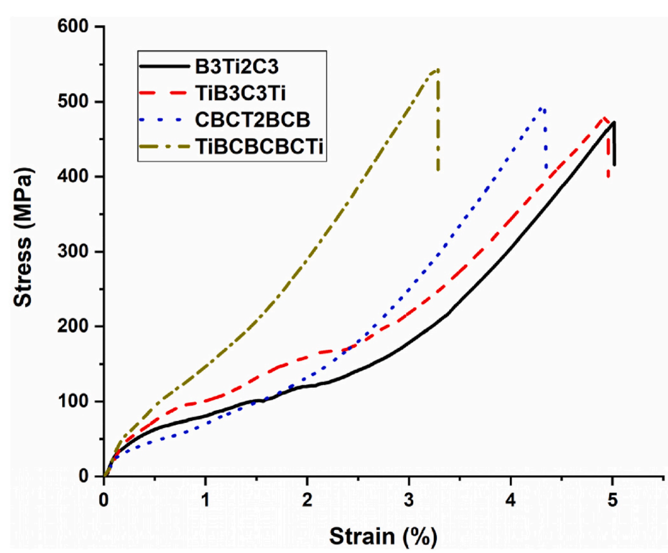

Fig. 5. Typical stress-strain curves of the various MFL composite samples.

accelerated crack propagation. The basalt fiber layer, having higher elongation, continued to bear the load until it reached an ultimate strain, leading to two fracture peaks in the force–displacement curve and indicating a dual fracture process [38].

However, within the MFL-IV structure, there was no double fracture. Among the goals of the experiment was to evaluate how the position of high-strength and low-strength fibers affected their overall mechanical properties. The carbon fiber-stacked composite exhibited the highest stiffness among all MFL composites, due to the superior interfacial adhesion between high-strength carbon fiber and matrix. The stress-strain curves for the C/B/Ti hybrid composites displayed two distinct slopes during the tensile phase. In line with previous studies [34,35], a significant observation was the appearance of two tensile force peaks in the force–displacement curves of MFL-III and MFL-IV. Fracture analysis revealed that the carbon fiber layer fractured first, due to its lower elongation when compared with basalt fiber. The concentrated stress around the fractured carbon fibers accelerated crack propagation. The basalt fiber layer, with higher elongation, continued to bear the load until it reached an ultimate strain, leading to two fracture peaks, indicating a dual fracture process [38]. However, the MFL-IV structure did not exhibit double fractures, as each interface consisted of a single contact layer between carbon and basalt fibers. Moreover, the strain to failure decreased with a rise in basalt layers, due to the slight increase in brittleness of the composite caused by basalt fiber. In addition, the elasticity of MFL composites was assessed by estimating the strength of the outermost fiber layers in conjunction with the elasticity of the tensile curvature. This finding aligns with the study reported by Karuppasamy et al. [11], which demonstrated that composites with glass fiber in the outer layers exhibited higher tensile strengths.

The shattered surfaces of the tensile fractured MFL stacked composite samples are shown in Fig. 6(a)–(d). MFL with C/B/Ti composites showed fiber pullout, destruction, separation and separation from the epoxy matrix. The longitudinal orientation of the B3Ti2C3 composite exhibited fiber split and delamination, as depicted in Fig. 6(a).

The B3Ti2C3 composite, on the other hand, exhibited a poorerfiber-matrix bond, leading to fiber pullout and gap development when compared with the pure carbon combination, as shown by the fractured surface. The TiB3C3Ti design recorded similar failure characteristics to the B3Ti2C3 design, including fiber breakage, as depicted in Fig. 6(b). Furthermore, according to Fig. 6(c), fiber breakage was observed in the longitudinal direction within the CBCTI2BCB composite. This response was consistent with prior work on the outermost fracture of hybrid composites made from natural fibers and polymers [20].From Fig. 6(d), fiber pullout was observed in the transfer direction and matrix crack within the CBCTI2BCB composite.

3.2. Flexural strengths of the woven MFL composites

The effects of various fiber stacking configurations on the flexural strength (FS) of the various composite samples are depicted in Fig. 7. Due to the strength of the carbon fiber, the composite with a pure carbon core and an outside layer of Ti mesh (TiC6Ti) recorded the maximum FS among the MFL composites [26]. The stacking sequences of both MFL-I and MFL-II composites had a major impact on their FS, which depended on the different and location of titanium, basalt and carbon fabric layers.

When compared with the TiB6Ti composite with Ti mesh skin and a basalt fabric core, the TiC6Ti composite with high-strength carbon fiber layers showed greater FS. The outside woven skin layer significantly impacted the tensile strength of the MFL-II sample. The FS of carbon-stacked Ti composites was higher than that of basalt-stacked Ti composites, demonstrating a similar tendency. However, the FS of composites containing a Ti core decreased. The FS of MFL-III and MFL-IV hybrid fiber-stacked composites differed according to the locations of their core and fiber. When compared with B3Ti2C3, TiB3C3Ti and CBCTi2CBC stacking configurations, the TiBCBCBCTi composite with an interwoven laminate demonstrated a highest FS. Among them, the CBCTi2CBC composite outperformed B3Ti2C3 and TiB3C3Ti in terms of tensile strength. Strong interfacial adhesion was responsible for the

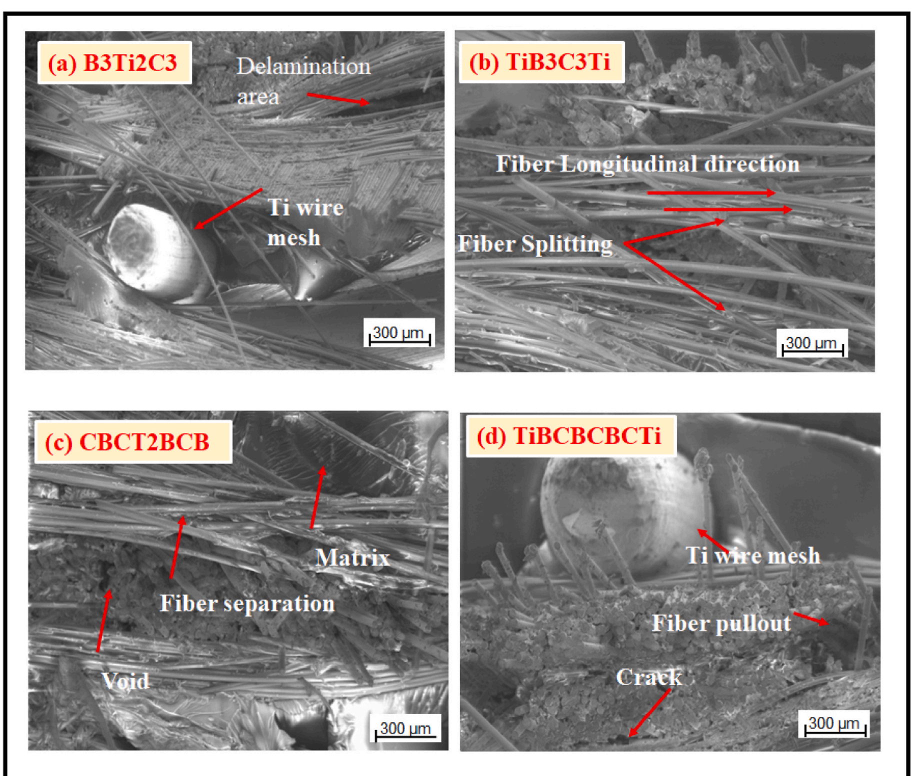

Fig. 6. SEM images of typical tensile fractured surfaces of B/C/Ti hybrid composites.

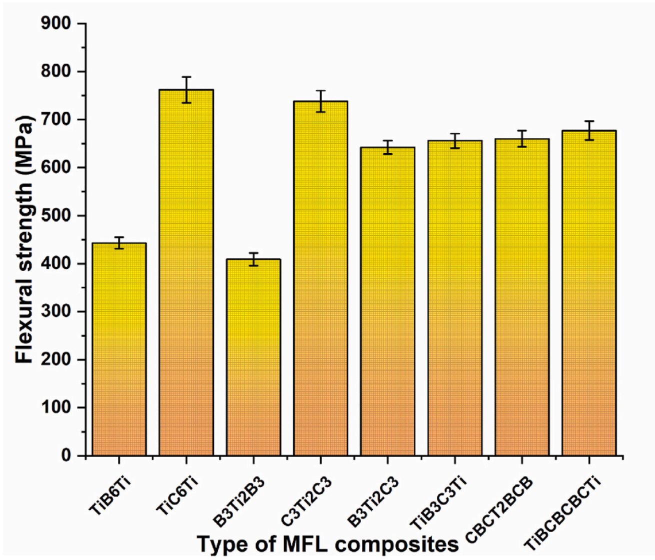

Fig. 7. Flexural strengths of the various stacked MFL-I, –II, –III and -IV polymer composites.

enhanced bending strength in alternate fiber stacking patterns [23].

3.3. Impact strengths of the woven MFL composites

Based on the impact test results of the polymer composites, it was evident that the highest energy dissipation occurred in the hybrid MFL-reinforced composites. As depicted in Fig. 8, the impact strengths of the stacked woven MFL composites varied significantly, depending on the type and arrangement of their reinforcements. A notable enhancement in impact strength was observed when basalt and Ti wire mesh fibers were combined within the composite structure. Among all tested configurations, the composites reinforced with six layers of basalt fiber exhibited the highest impact strength. Specifically, the carbon-intertwined basalt MFL composites demonstrated a range of impact strength values, with the minimum and maximum recorded at 183 and 204 kJ/m^2, respectively. These values indicated that the hybrid composites outperformed the composites reinforced with pure basalt fibers

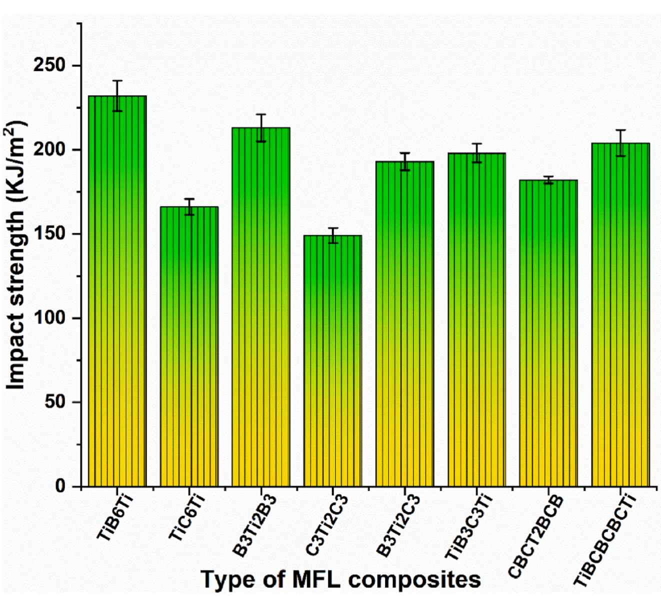

Fig. 8. Impact strengths of the various stacked MFL-I, –II, –III and-IV polymer composites.

alone. The performance of the best hybrid configurations approached, and in some cases exceeded, the impact strengths of the pure basalt fiber composites, confirming the synergistic effect of hybridization [11].

Furthermore, when comparing the different hybrid configurations, the alternate stacking sequence of basalt and carbon fibers reinforced with wire mesh, identified as TiBCBCBC, exhibited the highest impact strength among all woven MFL composite arrangements. This suggests that the specific stacking sequence and the balanced distribution of carbon and basalt fibers within the composite matrix contributed significantly to the energy absorption under impact loading. The enhanced performance can be attributed to improved stress distribution, crack deflection mechanisms and fiber bridging provided by the hybrid and alternating fiber structure.

3.4. Dynamic mechanical analysis of the woven MFL composites

3.4.1. Storage modulus

During DMA, the storage modulus is a crucial parameter that must be considered, as it determines the quantity of energy absorbed through a material throughout each oscillation period at a particular temperature. The stiffness of viscoelastic materials is associated with the storage modulus.Temperature- and frequency-induced fluctuations in the storage modulus of Ti wire mesh affected the mechanical and thermo-mechanical properties of B/C stacked Ti fiber laminates (Fig. 9).

In other words, Fig. 9 shows the differences in storage moduli of the various hybridized woven multilayer B/C/Ti MFL hybrid composites at frequency of 1.0 Hz and various temperatures. It was observed that the first or upper skin of basalt fiber in B3Ti2C3 laminate reduced storage modulus of 5967.9 MPa (nearly 22 %) when compared with similar C3Ti2C3 sample, establishing the higher performance of synthetic carbon fiber when compared with natural basalt fiber. As further shown in Fig. 9, the TiB3C3Ti (MFL-III) composite samples exhibited a larger storage modulus till around temperature of 90 °C than the CBCT2BCB (MFL-IV) composite, although they and other samples with total carbon plies of three were somewhat similar after 90 °C.

Moving forward, the storage modulus of DMA increased by adding a strong-stiffness carbon layer to the composite.Glassy and rubbery are two distinct zones that polymer composites frequently exhibit, as the testing temperature rises. Fiber-reinforced polymer composites typically have a high storage modulus prior to reaching the glassy state [32]. Under this condition; the rigidity of the composite components keeps the polymer chains stationary.However, as the polymer chains gain mobility in the rubbery state, the storage modulus declines progressively,

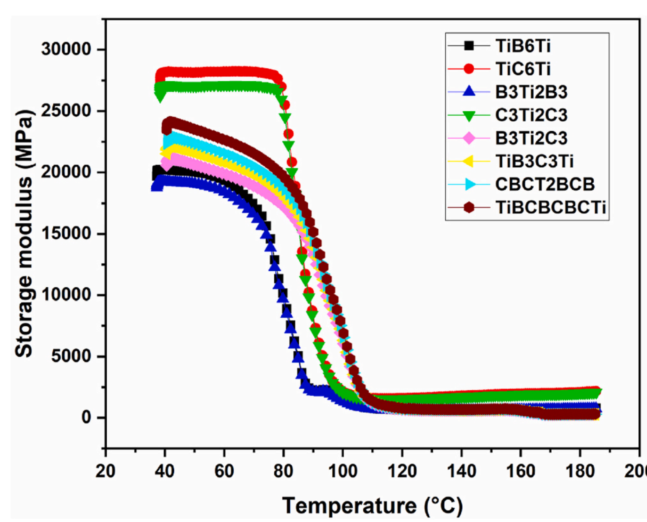

Fig. 9. Storage moduli of the various B/C/Ti MFL hybrid polymer composite samples.

particularly at elevated temperatures, resulting in a reduction of the elasticity of the composites.The ability to move polymer chains in a composite is determined by the type of fibers and their stacking sequences.The dynamic mechanical properties of composite laminates are significantly influenced by the position and interweaving pattern of weak-strength carbon and strong basalt fibers [30].

At 1.0 Hz, Table 2 presents the dynamic properties of the different woven layered patterns MFL-I, –II, –III and -IV of the entangled composite samples. The storage moduli, dampening values and loss moduli of the various samples were examined. The maximum or optimal storage modulus of 28185.2 MPa was obtained in the MFL-I (TiC6Ti) with exceptionally strong bond between Ti and carbon (C6) stacked composite. The influence of stacking sequence on DMA behavior can be attributed to the hierarchical confinement imposed by the alternating carbon, basalt and titanium layers. Carbon/Ti-rich configurations (such asTiC_6Ti) generated rigid interfacial constraint zones that suppressed segmental α-relaxation of the epoxy, reducing damping and increasing storage modulus. In contrast, basalt-rich sequences introduced compliant interfaces that enhanced localized chain mobility and interfacial friction, yielding higher tan δ values. Alternating fiber stacks (TiBCBCBCTi) created multiple stiffness gradients that produced distributed relaxation times and moderate damping. Thus, stacking sequence modulated viscoelastic behavior through spatial variations in molecular confinement and interfacial free volume, not merely through macroscopic stiffness differences. Hence, sample TiC6Tiinterleaved laminate pattern in MFL-I samples showed a greater storage modulus than the TiB6Tiwoven layered design, suggesting that the addition of carbon increased the storage elasticity more than basalt. This conclusion was similar to Doddi et al. [22], who studied palm/basalt hybrid composites. A connection of the exceptionally resistant carbon skin layer and the surrounding polymer matrix restricted the polymeric chain to move can be similarly observed in MFL-II, resulting in an improved storage modulus. Moreover, the skin wire mesh design (MFL-I) and alternate basalt and carbon fiber configuration (MFL-II) effectively controlled the movement of molecular chains, thereby enhancing the storage modulus linked to carbon fiber-based composites.

3.4.2. Loss modulus

The proportion of polymeric chain mobility rises with temperature, enabling the chains to travel more easily, especially in the vicinity of the glass transition (Tg) region. The enhanced mobility effects in a characteristic peak in the loss modulus, indicating maximum energy dissipation at Tg. The loss modulus values and associated temperatures for stacked MFL composites under oscillatory frequency of 1.0 Hz are shown in Fig. 10. The energy absorbed during molecular oscillations is largely influenced by the quality of interfacial bonding between the polymer matrix and the reinforcing fibers. In composites, such as B3Ti2C3, TiB3C3Ti and CBCTi2CBC, their loss moduli were moderately affected by the strong interactions between the matrix and basalt fibers [22]. Consequently, the loss modulus peaks in these basalt-reinforced composite samples are slightly lower in intensity when compared with those observed in the MFL composites with higher six carbon plies. On the other hand, composites with a greater number of carbon fiber layers, such as TiB6Ti and B3Ti2B3, display even lower peak intensities in the loss modulus, indicating reduced interfacial friction and energy dissipation.

Table 2
Dynamic mechanical investigation of MFL-I, –II, –III and-IV composites at 1.0 Hz.

Description	Type of layering composites	Storage modulus (MPa)	Loss modulus (MPa)	Tan delta
MFL-I	TiB6Ti	20244.70	3753.40	0.67
	TiC6Ti	28185.20	5333.60	0.49
MFL-II	B3Ti2B3	19280.70	3543.15	0.72
	C3Ti2C3	27127.30	5226.37	0.45
MFL-III	B3Ti2C3	21159.40	3900.15	0.63
	TiB3C3Ti	22130.10	4077.43	0.58
MFL-IV	CBCT2BCB	22973.00	4527.09	0.64
	TiBCBCBCTi	24121.80	4889.25	0.57

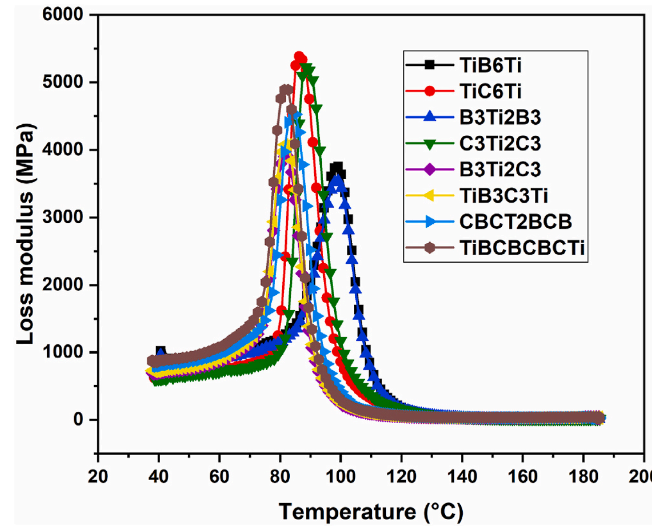

Fig. 10. Loss moduli of the various C/B/Ti MFL hybrid polymer composite samples.

Table 2 previously presents the loss moduliunder frequency of 1.0 Hz across different woven layered configurations MFL-I, –II, –III and -IV. In MFL-I composites, the loss modulus of TiC6Ti arrangement exceeded that of TiB6Ti laminate, indicating that the carbon layers enhanced the loss modulus by constraining polymer chains [22]. The decrease in peak height increased to the glass temperature of transition (Tg), revealing that the polymer chain was significantly immobilized by an interwoven structure [22].The loss modulus dropped with temperature after Tg, due to the unhindered flow of polymer molecules in the glassy region. When compared with the previous stacking layering arrangement, the loss factor of the basalt-carbon interlaced composite sample TiCBCBCBTi was higher.

3.4.3. Tan delta

The change in the loss modulus of the storage modulus ratio of viscoelastic materials when exposed to cyclical vibrations at a specific frequency is known as damping or tan delta. It stands for the amount of energy lost during the vibration.The tan delta fluctuations of the various MFL stacked composites at various testing temperatures is shown in Fig. 11. Considering Fig. 11, the lowest damping values are obtained by C3Ti2C3and TiC6Ti stacking sequences with strong stiffness and no appreciable loss of modulus of storage up to Tg. Tan delta can be decreased in polymer composites reinforced with strong-stiffness fibers. However, fracture surface investigation demonstrated that weak interfaces result in higher internal dissipation energy, which established the reason why damping values were increased or highest for B3Ti2B3 and followed byTiB6Ti stacking designs. Damping characteristics of all MFL composites dropped steadily with temperature after attaining Tg [26,28]. At increasing temperatures, stiffness relaxes, allowing polymer chains to flow easier.

When subjected to cyclic vibration at a certain frequency, the damping or tan delta, of viscoelastic substances is determined by the proportion of a change in loss modulus to storage modulus. In addition, Table 2 presents the tan delta estimates for the various composite designs. In MFL-I composites, the damping peak was smaller for the carbon fiber stacking design (TiC6Ti) than for the basalt fiber counterpart. Due to their inherent porosity, carbon strands have the potential to release energy.In MFL-II, the skin basalt configuration that included additional Ti levels in the core layering configuration, sample B3Ti2B3 recorded

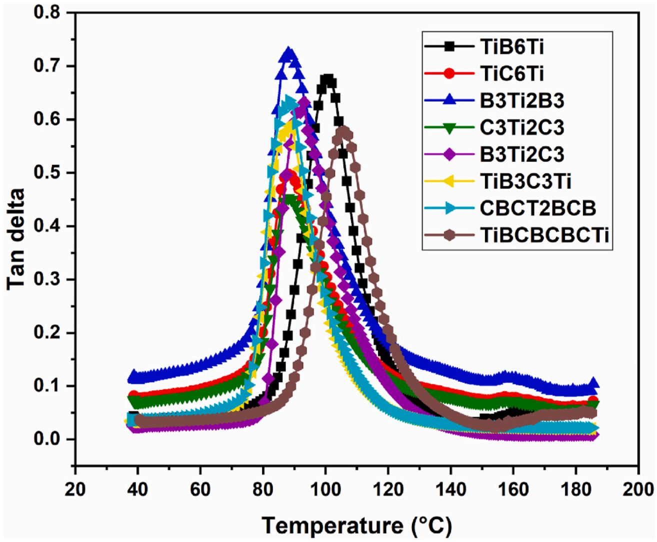

Fig. 11. Tan delta of the various C/B/Ti MFL hybrid polymer composite samples.

the higher damping value of 0.72 when compared with TiC6Ti design with 0.49.Composite materials comprised of natural fibers lose some of their dampening properties when carbon fiber was added, since it increases both elasticity and robustness of the materials.

Sample TiB3C3Ti, which has equal inner layers of both carbon and basalt fibers and an outside layer of Ti wire fiber mesh recorded better tan delta when compared with similar sample B3Ti2C3. Therefore, it has improved damping behavior in MFL-III composites. Importantly, the arrangement of the fiber determined the damping properties of the various MFL composites. This was obvious between the samples under MFL-IV, whereby sample TiBCBCBCTi performed better than CBCT2BCB counterpart, despite of having the same layers or plies of fibers (two Ti, three C and three B). The Tg of the interwoven composites increased by the improved thermal durability of the carbon fibers. The alternative skin basalt-carbon multilayered composite sample TiBCBCBCTi had a higher Tg value of over 100 °C when the damping peaks were compared with sample CBCT2BCB. Its damping value of 0.57 was lower than that of the sample CBCT2BCBwith 0.64 [22].From the quantitative results obtained, it can be deduced that carbon-rich laminates (TiC_6Ti) achieved the highest tensile 0f ~ 612 MPa and flexural strength of ≈762 MPa, failing mainly by brittle fibre fracture. Basalt-rich laminates (samples TiB_6Ti and $B_3Ti_2B_3$) exhibited lower strengths of ≈389–443 MPa, but higher impact energy of ≈232 kJm^{-2} and damping (tan δ of ≈0.72), dominated by fibre pull-out and delamination. These trends indicated that carbon-rich systems suit stiffness-critical structures, while basalt-rich counterparts are preferred for impact or damping applications. Hybrid stacking (such as TiBCBCBCTi) offered balanced performance, and using Ti as outer skin enhanced load-bearing capability.The experimental results were validated through replicate testing (standard deviation < 5 %) and benchmarked against literature values for carbon–basalt and carbon–metal laminates. The measured tensile (612 MPa) and flexural (762 MPa) strengths, as well as the storage modulus (28.2 GPa), closely match reported data and theoretical rule-of-mixtures predictions. These consistencies confirmed that the performance improvements weregenuine, and validated the reliability of the experimental outcomes.

Overall, the mechanical and dynamic characteristics of the Ti wire mesh stacked with carbon fiber interwoven compositesamples C3Ti2C3 and TiC6Tiunder MFL-I and –II, respectively were satisfactory. As a substitute forbasalt-woven layer stacking composite, carbon interwoven skin can provide superior strength and thermal resistance.The carbon-based interface is very competitive in research, due to its advantageous qualities.However, direct quantification of interfacial bonding, such asinterlaminar shear strength (ILSS)and pull-out tests were not conducted. Since all composites received identical surface treatments, the observed differences in mechanical properties can be attributed primarily to stacking sequence effects rather than surface modification. Qualitative SEM analysis supported the conclusion that surface roughening and stress relief from annealing improved local adhesion, but future studies will include quantitative interfacial testing to validate and expatiatetheresults obtained. Although, there was no dedicated ILSS or pull-out test performed, but the uniform treatment of all Ti meshes established that the variations observed in tensile and flexural strengths can be predominantly attributed to both stacking sequence and fiber architecture. The interfacial enhancement from sandblasting and annealing was therefore considered as a constant precondition across all samples rather than a variable factor.

4. Conclusions

The influences of addition Ti wire mesh on both mechanical (tensile, flexural and impact strengths) and thermomechanical (tan delta/ damping, storage and loss moduli) of various stacking sequenced B/ CFRP hybrid composites have been investigated. From the results obtained and discussed, the following concluding remarks can be deduced.

- The TiC6Ti composite sample, comprising high-strength carbon fiber layers, demonstrated highest tensile strength of 612 MPa, followed by sample C3Ti2C3 when compared with other B/C/Ti MFL hybrid composite samples. Significantly, both samples had no basalt fiber; therefore, lowest tensile strengths of 409 and 389 MPa were recorded with samples TiB6Ti and B3Ti2B3 with highest layers or plies of basalt fibers, respectively.
- The TiC6Ti laminate exhibited excellent mechanical strength and stiffness, comparable to standard aerospace CFRPs and commercial FMLs, confirming its potential for highperformance structural applications.
- Similarly, the same sample TiC6Ti exhibited maximum flexural strength of over 750 MPa, followed by sample C3Ti2C3 when compared with other B/C/Ti MFL hybrid composite samples. However, lowest flexural strengths of approximately 443 and 409 MPa were recorded with samples TiB6Ti and B3Ti2B3, respectively. However, sample TiBCBCBCTi recorded the highest flexural strength among basalt fiber-based MFL hybrid composite samples.
- Among all tested configurations, the composites reinforced with six layers of basalt fiber; samples TiB6Ti exhibited the highest impact strength of 232 kJ/m2, followed by sample B3Ti2B3. However, the minimum impact strength was recorded at 149 kJ/m^2 by sample C3Ti2C3 without basalt fiber, followed by sample TiC6Ti, establishing the negative effect of absence of basalt fiber on the Ti MFL composite systems.
- Based on DMA, sample TiC6Ti recorded maximum storage and loss moduli of 28185.20 and 5333.60 MPa respectively, followed by sample C3Ti2C3 with storage and loss moduli of 27127.30 and 5226.37 MPa, respectively and lowest damping property with tan delta value of 0.45. However, sample B3Ti2B3 exhibited lowest storage and loss moduli of 19280.70 and 3543.15 MPa respectively, having poorest damping response or highest tan delta of 0.72.
-The developed basalt–carbon–titanium laminates demonstrated high tensile (612 MPa), flexural (762 MPa), and impact (166 kJ/m^2) strengths, coupled with excellent stiffness (storage modulus = 28.2 GPa) and low damping (tan δ = 0.45). These properties qualify them for structural and energy-absorbing applications such as aircraft panels, automotive bumpers, and helmets. Their strong interfacial bonding and vibration-damping capability indicate potential for lightweight, durable hybrid structures. However, full industrial adoption will require further fatigue, impact tolerance, environmental aging, and adhesion testing to establish long-term reliability

and compliance with aerospace and automotive certification standards.
- Applicably, both mechanical and thermomechanical properties obtained from the optimal B/C/Ti MFL interlaced composites established their suitability for machine components, including silencer guards for two-wheelers, various interior parts of vehicles, bus panels and structural parts, to mention but a few applications.

However, only flat laminate samples were fabricated and tested under standard ASTM standards in this study; no component-level parts were produced. Their suitability for aforementioned applications is based on mechanical and thermomechanical performance indicators. Future work will focus on prototype fabrication and application-specific tests, including fatigue, thermal cycling, vibration and acoustic evaluations to confirm their real-life applications and performances.

Declaration of competing interest

The authors declare that they have no known competing financial interests or personal relationships that could have appeared to influence the work reported in this paper.

Acknowledgement

The authors acknowledge the funding from the Ongoing Research Funding Program (ORF-2025-355), King Saud University, Riyadh, Saudi Arabia.

References

[1] Kormanikova E, Zmindak M, Novak P, Sabol P. Tensile properties of carbon fiber reinforced polymer matrix composites: application for the strengthening of reinforced concrete structure. Compos Struct 2021;275:114448.
[2] Ojha S, Bisaria H, Mohanty S, Kanny K. Fractographic analysis of fiber-reinforced polymer laminate composites for marine applications: a comprehensive review. Polym Compos 2024;45(8):6771–87.
[3] Hamzat AK, Murad MS, Adediran IA, Asmatulu E, Asmatulu R. Fiber-reinforced composites for aerospace, energy, and marine applications: an insight into failure mechanisms under chemical, thermal, oxidative, and mechanical load conditions. Adv Compos Hybrid Mater 2025;8(1):1–57.
[4] Kasi E, Ramasamy S, Kirubakaran R, Munusamy R, Sudalaimani EE, Karuppasamy A. Tensile, dynamic mechanical, and vibration behavior of layering sequence design effect of glass intertwined natural kenaf woven polymeric laminates. J Nat Fibers 2024;21(1):2316791.
[5] Zheng H, Zhang W, Li B, Zhu J, Wang C, Song G, Wu G, Yang X, Huang Y, Ma L. Recent advances of interphases in carbon fiber-reinforced polymer composites: a review. Compos B Eng 2022;233:109639.
[6] Rajak DK, Wagh PH, Linul E. Manufacturing technologies of carbon/glass fiber-reinforced polymer composites and their properties: a review. Polymers 2021;13 (21):3721.
[7] Sayam A, Rahman AM, Rahman MS, Smriti SA, Ahmed F, Rabbi MF, Hossain M, Faruque MO. A review on carbon fiber-reinforced hierarchical composites: mechanical performance, manufacturing process, structural applications and allied challenges. Carbon Lett 2022;32(5):1173–205.
[8] Lionetto F. Carbon fiber reinforced polymers. Materials 2021;14(19):5545.
[9] Seo J, Kim DC, Park H, Kang YS, Park HW. Advancements and challenges in the carbon fiber-reinforced polymer (CFRP) trimming process. Int J Precis Eng Manuf 2024;11(4):1341–60.
[10] Kumar A, Dixit S, Singh S, Sreenivasa S, Bains PS, Sharma R. Recent developments in the mechanical properties and recycling of fiber-reinforced polymer composites. Polym Compos 2025;46(5):3883–908.
[11] Karuppasamy A, Kirubakaran R, Gopalan V, Munusamy R, Krishnasamy K. Influences of basalt fiber position and addition on the mechanical and viscoelastic behaviors of steel mesh/flax/basalt fiber metal laminates. Iran Polym J (Engl Ed) 2024:1–13.
[12] Masud M, Mubashar A. Effect of hybridization on the mechanical performance and cost efficiency of carbon/flax bio-hybrid composites. Polym Compos 2024;45(11): 9766–84.
[13] Premnath K, Arunprasath K, Sanjeevi R, Elilvanan R, Ramesh M. Natural/Synthetic fiber reinforced hybrid composites on their mechanical behaviors–a review. Interactions 2024;245(1):111.
[14] Wang Y, Sun W, Cao L. Tensile and flexural mechanical attributes of hybrid carbon/basalt fiber metal laminates under various hybridization and stacking sequences. Compos Appl Sci Manuf 2024;177:107942.
[15] Ramraji K, Rajkumar K, Subbiah M, Balachandar K, Kumar PS. Stacking layer effect on mechanical and vibration behaviour of woven glass intertwined with kenaf fiber polymeric composites. Mater Today Proc 2022;62:1356–60.
[16] Dhand V, Mittal G, Rhee KY, Park SJ, Hui D. A short review on basalt fiber reinforced polymer composites. Compos B Eng 2015;73:166–80.
[17] Jagadeesh P, Rangappa SM, Siengchin S. Basalt fibers: an environmentally acceptable and sustainable green material for polymer composites. Constr Build Mater 2024;436:136834.
[18] Wang S, Zhong J, Gu Y, Li G, Cui J. Mechanical properties, flame retardancy, and thermal stability of basalt fiber reinforced polypropylene composites. Polym Compos 2020;41(10):4181–91.
[19] Fragassa C, Pavlovic A, Santulli C. Mechanical and impact characterisation of flax and basalt fiber vinylester composites and their hybrids. Compos B Eng 2018;137: 247–59.
[20] Keerthi Gowda BS, Naresh K, Ilangovan S, Sanjay MR, Siengchin S. Effect of fiber volume fraction on mechanical and fire resistance properties of basalt/polyester and pineapple/polyester composites. J Nat Fibers 2022;19(13):6074–88.
[21] Ramraji K, Rajkumar K, Sabarinathan P. Mechanical and free vibration properties of skin and core designed basalt woven intertwined with flax layered polymeric laminates. Proc IME C J Mech Eng Sci 2020;234(22):4505–19.
[22] Das SC, Paul D, Grammatikos SA, Siddiquee MA, Papatzani S, Koralli P, Islam JM, Khan MA, Shauddin SM, Khan RA, Vidakis N. Effect of stacking sequence on the performance of hybrid natural/synthetic fiber reinforced polymer composite laminates. Compos Struct 2021;276:114525.
[23] Amico SC, Angrizani CC, Drummond ML. Influence of the stacking sequence on the mechanical properties of glass/sisal hybrid composites. J Reinforc Plast Compos 2010;29(2):179–89.
[24] Aabdul Khalil HPS, Kang CW, Khairul A, Ridzuan R, Adawi TO. The effect of different laminations on mechanical and physical properties of hybrid composites. J Reinforc Plast Compos 2009;28(9):1123–37.
[25] Doddi PRV, Chanamala R, Dora SP. Effect of fiber orientation on dynamic mechanical properties of PALF hybridized with basalt reinforced epoxy composites. Mater Res Express 2020;7(1):015329.
[26] Monte Vidal DCDS, Ornaghi Jr HL, Ornaghi FG, Monticeli FM, Voorwald HJC, Cioffi MOH. Effect of different stacking sequences on hybrid carbon/glass/epoxy composites laminate: thermal, dynamic mechanical and long-term behavior. J Compos Mater 2020;54(6):731–43.
[27] Samson PE, Kumaran SS, Shanmugam V, Das O. The effect of fiber orientation and stacking sequence on carbon/Kevlar/epoxy intraply hybrid composites under dynamic loading conditions. Polym Adv Technol 2023;34(5):1585–98.
[28] Pathak AK, Garg H, Subhedar KM, Dhakate SR. Significance of carbon fiber orientation on thermomechanical properties of carbon fiber reinforced epoxy composite. Fibers Polym 2021;22:1923–33.
[29] Romanzini D, Ornaghi Jr HL, Amico SC, Zattera AJ. Influence of fiber hybridization on the dynamic mechanical properties of glass/ramie fiber-reinforced polyester composites. J Reinforc Plast Compos 2012;31(23):1652–61.
[30] Azimpour-Shishevan F, Akbulut H, Mohtadi-Bonab MA. Mechanical and thermal properties of carbon/basalt intra-ply hybrid composites. I. Effect of intra-ply hybridization. Fibers Polym 2020;21(11):2579–89.
[31] Yang H, Ng BC, Yu HC, Liang HH, Kwok CC, Lai FW. Mechanical properties study on sandwich hybrid metal/(carbon, glass) fiber reinforcement plastic composite sheet. Adv Compos Hybrid Mater 2022:1–8.
[32] Prakash VA, Jaisingh SJ. Mechanical strength behaviour of silane treated E-glass fiber/Al 6061 & SS-304 wire mesh reinforced epoxy resin hybrid composite. Silicon 2018;10:2279–86.
[33] Costa RD, Sales-Contini RC, Silva FJ, Sebbe N, Jesus AM. A critical review on fiber metal laminates (FML): from manufacturing to sustainable processing. Metals 2023;13(4):638.
[34] Xiao H, Sultan MTH, Shahar FS, Gaff M, Hui D. Recent developments in the mechanical properties of hybrid fiber metal laminates in the automotive industry: a review. Rev Adv Mater Sci 2023;62(1):20220328.
[35] Krishnasamy P, Rajamurugan G, Thirumurugan M. Performance of fiber metal laminate composites embedded with AL and CU wire mesh. J Ind Textil 2022;51(4_suppl):6884S–901S.
[36] Bin Salim MY, Farokhi Nejad A, Yahya MY, Dickhut T, Rahimian Koloor SS. Mechanical characterization of hybrid steel wire mesh/basalt/epoxy fiber-reinforced polymer composite laminates. J Compos Sci 2024;8(5):184.
[37] Botelho EC, Silva RA, Pardini LC, Rezende MC. A review on the development and properties of continuous fiber/epoxy/aluminum hybrid composites for aircraft structures. Mater Res 2006;9:247–56.
[38] Huang Y, Sultan MTH, Shahar FS, Łukaszewicz A, Oksiuta Z, Grzejda R. Kenaf fiber-reinforced biocomposites for marine Applications:AReview. Materials 2025; 18:1–32.
[39] Shelly D, Singhal V, Jaidka S, Banea MD, Lee S-Y, Park S-J. Mechanical performance of bio-based fiber reinforced polymer composites: a review. Polym Compos 2025:1–35.
[40] Abdul Ghafar AS, Hajjaj SSH, GsangayaK R, Sultan MTH, Mail MF, Hua LS. Design and development of a robot for spraying fertilizers and pesticides for agriculture. Mater Today Proc 2023;81(Part 2):242–8.
[41] Harsha MS, Kumar VSH, Prasad MB, Muthukumar C, Thiagamani SMK, Ayrilmis N, Krishnasamy S, Ng LF, Jesuarockiam N. Synergistic effects of titanium dioxide and graphene nanofillers on delamination and thrust forces in machining glass fiber reinforced nanocomposites. Sci Rep 2025;15(1). https://doi.org/10.1038/s41598-025-92140-3.